

This is the accepted manuscript made available via CHORUS. The article has been published as:

Indirect determination of the astrophysical S factor for the ${}^6\text{Li} + \text{p} \rightarrow \text{Be} + \gamma$ reaction using the asymptotic normalization coefficient method

G. G. Kiss et al.

Phys. Rev. C **104**, 015807 — Published 29 July 2021

DOI: [10.1103/PhysRevC.104.015807](https://doi.org/10.1103/PhysRevC.104.015807)

Indirect determination of the astrophysical S-factor for the ${}^6\text{Li}(p, \gamma){}^7\text{Be}$ reaction using the asymptotic normalization coefficient (ANC) method

G. G. Kiss,^{1,*} M. La Cognata,^{2,†} R. Yarmukhamedov,^{3,‡} K. I. Tursunmakhatov,^{3,4} I. Wiedenhöver,⁵ L. T. Baby,⁵ S. Cherubini,^{2,6} A. Cvetinović,² G. D'Agata,⁷ P. Figuera,² G. L. Guardo,^{2,6} M. Gulino,^{2,8} S. Hayakawa,⁹ I. Indelicato,^{2,6} L. Lamia,^{2,6,10} M. Lattuada,^{2,6} F. Mudò,^{2,6} S. Palmerini,^{11,12} R. G. Pizzone,² G. G. Rapisarda,^{2,6} S. Romano,^{2,6,10} M. L. Sergi,^{2,6} R. Sparta,^{2,6} C. Spitaleri,^{2,6} O. Trippella,^{11,12} A. Tumino,^{2,8} M. Anastasiou,⁵ S.A. Kuvin,⁵ N. Rijal,⁵ B. Schmidt,⁵ S. B. Igamov,³ S. B. Sakuta,¹³ Zs. Fülöp,¹ Gy. Gyürky,¹ T. Szücs,¹ Z. Halász,¹ E. Somorjai,¹ Z. Hons,⁷ J. Mrázek,⁷ R. E. Tribble,¹⁴ and A. M. Mukhamedzhanov¹⁴

¹*Institute for Nuclear Research (ATOMKI), H-4001 Debrecen, POB.51, Hungary*

²*Laboratori Nazionali del Sud - INFN, Via S. Sofia 62, 95123 Catania, Italy*

³*Institute of Nuclear Physics, Uzbekistan Academy of Sciences, 100214 Tashkent, Uzbekistan*

⁴*Physical and Mathematical Department, Gulistan State University, 120100 Gulistan, Uzbekistan*

⁵*Department of Physics, Florida State University, Tallahassee, Florida 32306, USA*

⁶*Dipartimento di Fisica e Astronomia "E. Majorana", Università di Catania, 95123 Catania, Italy*

⁷*Nuclear Physics Institute of the Czech Academy of Sciences, 250 68 Řež, Czech Republic*

⁸*Facoltà di Ingegneria e Architettura, Università di Enna "Kore", 94100, Enna, Italy*

⁹*Center for Nuclear Study (CNS), University of Tokyo, RIKEN campus, Saitama 351-0198, Japan*

¹⁰*Centro Siciliano di Fisica Nucleare e Struttura della Materia (CSFNMS), Catania 95123, Italy*

¹¹*Dipartimento di Fisica e Geologia, Università di Perugia, 06123 Perugia, Italy*

¹²*Istituto Nazionale di Fisica Nucleare, Sezione di Perugia, 06123 Perugia, Italy*

¹³*National Research Center "Kurchatov Institute", Moscow 123182, Russia*

¹⁴*Cyclotron Institute, Texas A&M University, College Station, Texas 77843, USA*

(Dated: June 30, 2021)

Background: The ${}^6\text{Li}(p, \gamma){}^7\text{Be}$ cross section influences a variety of astrophysical scenarios, including big bang and stellar nucleosynthesis. In recent years, conflicting results of direct measurements have been published, reporting contradictory low-energy trends.

Purpose: In order to shed light on the contradiction between the existing data sets, the reaction was studied using the asymptotic normalization coefficient (ANC) technique which was up-to-now never used for this reaction.

Methods: To derive the ANC, the ${}^6\text{Li}({}^3\text{He}, d){}^7\text{Be}$ transfer reaction, studied at the Department of Physics and Astronomy of the University of Catania and at the John. D. Fox Superconducting Accelerator Laboratory at the Florida State University, was re-analyzed focusing on the proton transfer mechanism [the α transfer process is discussed in G.G. Kiss et al., Phys. Lett. B 807, 135606 (2020)]. The energy of the ${}^3\text{He}$ beam impinging on a ${}^6\text{Li}$ target was $E_{\text{lab}} = 3$ MeV and $E_{\text{lab}} = 5$ MeV. The yield of the emitted deuterons was measured with high precision using silicon ΔE -E telescopes.

Results: From the DWBA analysis of the angular distributions of the emitted deuterons populating the ground ($E^* = 0.0$ MeV; $\frac{3}{2}^-$) and the first excited ($E^* = 0.429$ MeV; $\frac{1}{2}^-$) states of ${}^7\text{Be}$, the ANCs for the ${}^6\text{Li} + p \rightarrow {}^7\text{Be}$ system were deduced. Furthermore, the recently measured ${}^6\text{Li}(p, \gamma){}^7\text{Be}$ reaction cross sections [D. Piatti et al., Phys. Rev. C 102, 052802 (2020)] were also analyzed within this theoretical framework. Excellent agreement was found between ANC values derived indirectly and determined from the direct data, which strengthens the conclusion of the present work. The astrophysical S-factor — at energies characterizing the Sun — for the ${}^6\text{Li}(p, \gamma){}^7\text{Be}$ reaction was calculated using the weighted mean of the experimentally derived ANC values.

Conclusions: The result of the present comprehensive study supports the extrapolation of [D. Piatti et al., Phys. Rev. C 102, 052802 (2020); G.X. Dong et al., J. Phys. G Nucl. Partic. 44, 045201 (2017); A. Gnech and L.E. Marcucci, Nucl. Phys. A 987, 1 (2019)], thus disfavors the conclusions drawn in [J.J. He et al., Physics Letters B 725, 287 (2013); Y. Xu et al., Nucl. Phys. A 918, 61 (2013)].

I. THE ${}^6\text{Li}(p, \gamma){}^7\text{Be}$ REACTION: ASTROPHYSICAL ROLE AND CROSS SECTION INFORMATION

Understanding present-day light elements abundances represents one of the most intriguing topic in

astrophysics. Besides the role of D, ${}^3\text{He}$ and Li as tracers of the big bang nucleosynthesis (BBN), one has to take into account¹ the contribution of galactic cosmic-ray spallation leading to the synthesis of a large fraction of the observed Li, Be and B abundances [2].

* ggkiss@atomki.mta.hu

† lacognata@lns.infn.it

‡ Deceased

¹ Other contribution, in the special case of lithium, can be also due to neutrino-driven nucleosynthesis in supernovae explosions [1]

Focusing on lithium isotopes, less than half of the present solar system ${}^7\text{Li}$ supply is thought to be produced in the BBN, while a large fraction has been synthesized in stellar scenarios [3]. In the case of ${}^6\text{Li}$, the amount presently observed is almost exclusively produced by cosmic rays [4], and the possibility of a primordial ${}^6\text{Li}$ plateau, similar to the one for ${}^7\text{Li}^2$, is not presently confirmed (see [6] and references therein). It is believed that the $d(\alpha, \gamma){}^6\text{Li}$ reaction is the main source of ${}^6\text{Li}$ in the early Universe, the ${}^6\text{Li}(p, \alpha){}^3\text{He}$ and ${}^6\text{Li}(p, \gamma){}^7\text{Be}$ reactions being the foremost destruction channels [7, 8].

Since the production mechanism of ${}^6\text{Li}$ and ${}^7\text{Li}$ are completely different, the ${}^6\text{Li}/{}^7\text{Li}$ isotopic ratio can be used either to constrain the lithium production mechanisms and/or the galactic enrichment processes, e.g., the role played by cosmic-ray induced spallation [9] or by deep circulation in evolved stars [10], modifying the primordial ${}^7\text{Li}$ abundance. For this purpose, an accurate determination of the ${}^6\text{Li}(p, \gamma){}^7\text{Be}$ astrophysical S-factor is needed. Unfortunately, at present — as it is discussed in the following paragraphs — the available experimental data are contradictory. Furthermore, the experiments were performed typically at energies higher than the ones of astrophysical interest, therefore extrapolation is necessary. Moreover, the enhancement due to the electron screening effect [11] has also to be taken into account.

As it was proven in other cases, indirect techniques like Trojan Horse Method or asymptotic normalization coefficient (ANC) can give important clues to the understanding of BBN (e.g. ref.[12] for a review).

Despite its high importance, experimental cross section data on the ${}^6\text{Li}(p, \gamma){}^7\text{Be}$ reaction are scarce ([6] and references therein for the available data sets). The data set most commonly recommended [13] for astrophysical calculations is from 1979 [14] although the reported S-factor is affected by sizeable total uncertainty ($\sim 15\%$), making the theoretical description of the data challenging and the resulting extrapolation questionable.

In 2013, a new measurement was performed [15]. In that work a $J^\pi = (1/2^+, 3/2^+)$ state in ${}^7\text{Be}$ located at about 200 keV above the ${}^7\text{Be} \rightarrow p+{}^6\text{Li}$ threshold was suggested, but such resonance was not observed in the ${}^3\text{He}(\alpha, \gamma){}^7\text{Be}$ reaction at the corresponding energy [16]. This discrepancy triggered a new work of the LUNA collaboration [17], covering the energy region studied by [15]. In the LUNA experiment the ${}^6\text{Li}(p, \gamma){}^7\text{Be}$ astrophysical S-factor was determined using a relative approach, by normalization to the one of the ${}^6\text{Li}(p, \alpha){}^3\text{He}$ reaction. This novel measurement questions the presence of the resonance reported in [15], the new experimental data being characterized by a smoothly increasing S-factor towards lower energies. Electron screening effect was corrected for by following the adiabatic approxima-

tion described in ref. [11], in agreement with the indirect measurement [18].

The ${}^6\text{Li}(p, \gamma){}^7\text{Be}$ cross section was also calculated using different theoretical models (for summary see [6]). The list includes a potential model [19], a Gamow shell model [20], cluster models [6, 21] and R-matrix fits [15, 17, 22]. The results of the theoretical calculations can be sorted into two groups, either including or neglecting the contribution of the unconfirmed resonance. It is important to point out that the most recent calculation [6], performed with the cluster model, is able to reproduce the trend but not the absolute value of the non resonant S-factor, and accordingly a scaling factor is needed to match with the available experimental data.

As a consequence of the difficulties outlined above, the cross section (or equivalently the astrophysical S-factor) of the ${}^6\text{Li}(p, \gamma){}^7\text{Be}$ reaction is still known with large experimental uncertainties and the various extrapolated S-factors differ significantly (by about 30%), making it very hard to draw astrophysical conclusions. For this reason, in the present work the astrophysical $S_{61}(E)$ factor of the ${}^6\text{Li}(p, \gamma){}^7\text{Be}$ reaction was experimentally determined directly at solar energies, based on the ANC indirect method [23]. The aim of this method is to deduce the direct capture contribution to the radiative capture cross section and consequently the astrophysical factor, by using the ANC's which, in turn, are obtained by studying peripheral transfer reactions. The direct capture cross section of the ${}^6\text{Li}(p, \gamma){}^7\text{Be}$ reaction is proportional to the square of the ANC [24, 25] which can be determined experimentally via transfer reactions. In particular, the study of the near barrier proton transfer ${}^6\text{Li}({}^3\text{He}, d){}^7\text{Be}$ reaction allows to determine the ANCs in ${}^6\text{Li} + p \rightarrow {}^7\text{Be}$ for both the ground and first excited (0.429 MeV) states of the ${}^7\text{Be}$ nucleus. This independent experimental approach using the ANC indirect method, up-to-now never used to study the ${}^6\text{Li}(p, \gamma){}^7\text{Be}$ reaction, not only improves our understanding on the low energy behavior of this reaction but also helps to identify the hidden systematic uncertainties of the measurements performed so far. Furthermore, to increase the accuracy of the astrophysical S factor derived here, the the ANCs for the ${}^6\text{Li} + p \rightarrow {}^7\text{Be}(\text{g.s.})$ and ${}^6\text{Li} + p \rightarrow {}^7\text{Be}(0.429 \text{ MeV})$ channels, were derived from the experimental total astrophysical S-factor and the branching ratios of ref. [17], within the modified two body potential method (MTBPM) [26].

This paper is organized as follows. The experimental approach is presented together with details of the theoretical analysis in Sec. II. The extraction of the ANC parameters from the recently measured direct experimental ${}^6\text{Li}(p, \gamma){}^7\text{Be}$ cross sections [17] are discussed in Sec. III. Finally, the results and the consequences of the presented comprehensive study are given in Sec. IV.

² The so-called Spite-plateau refers to the constant ${}^7\text{Li}$ abundance as a function of metallicity observed in metal poor stars [5]

II. THE STUDY OF THE ${}^6\text{Li}({}^3\text{He},d){}^7\text{Be}$ TRANSFER REACTION AND THE DETERMINATION OF THE ANC FOR THE ${}^6\text{Li}(p,\gamma){}^7\text{Be}$ CAPTURE REACTION

A. Experimental details

To determine the ANCs for ${}^6\text{Li} + p \rightarrow {}^7\text{Be}$ ground and first excited states, the angular distributions of the deuterons emitted in the near barrier transfer reaction ${}^6\text{Li}({}^3\text{He}, d){}^7\text{Be}$ were measured in a broad angular interval — in particular, covering the forward hemisphere — in parallel with the sub-Coulomb alpha transfer. More details about the experiments are given in [27] and here only the most important aspects are summarized.

To do so, we used ${}^3\text{He}$ beams provided by the 3.5 MV singletron accelerator of the Department of Physics and Astronomy (DFA) of the University of Catania (Italy) and the FN tandem accelerator at the John D. Fox Superconducting Accelerator Laboratory at the Florida State University (FSU), Tallahassee (FL), USA. Angular distributions were measured at two energies ($E_{lab.} = 3$ MeV and $E_{lab.} = 5$ MeV) using silicon ΔE -E telescopes fixed on a remotely controlled turntable. Additional monitor detectors were placed at fixed angles with respect to the beam axis to check the target thickness and for normalization purpose. ${}^6\text{LiF}$ (enriched in ${}^6\text{Li}$ by 95%) and pure ${}^6\text{Li}$ targets (enriched in ${}^6\text{Li}$ by 98%) were made by vacuum evaporation on Formvar backings, with thicknesses ranging between 50-150 $\mu\text{g}/\text{cm}^2$. In both experiments, deuteron identification was achieved using the standard ΔE -E technique and the peak areas were derived by fitting Gaussian functions for d_0 and d_1 groups, corresponding to ${}^7\text{Be}$ ground and first excited states. A typical one-dimensional deuteron spectrum is presented in fig.1 (the peaks corresponding to the ${}^7\text{Be}$ ground and 1st excited state are marked with d_0 and d_1 , respectively). It can be seen that the separation of the different deuteron groups is sufficient to derive the yields for each reaction channel. The resulting angular distributions are shown in fig.2 as solid circles. Error bars include statistical, integration and normalization uncertainties.

Unlike work [27], where the break up process of ${}^6\text{Li}$ with the transfer of an alpha particle in the ${}^6\text{Li}({}^3\text{He},d){}^7\text{Be}$ reaction was investigated and therefore the cross sections at large angles were analysed, here attention is paid to study the break up of ${}^3\text{He}$ and measurements only in the region in the forward hemisphere, where the direct mechanism of proton transfer dominates.

B. Theoretical analysis and extraction of the ${}^6\text{Li}+p \rightarrow {}^7\text{Be}$ ANCs

The experimental data were analyzed in the framework of the modified Distorted-Wave Born Approximation (DWBA) approach [30]; the differential cross section

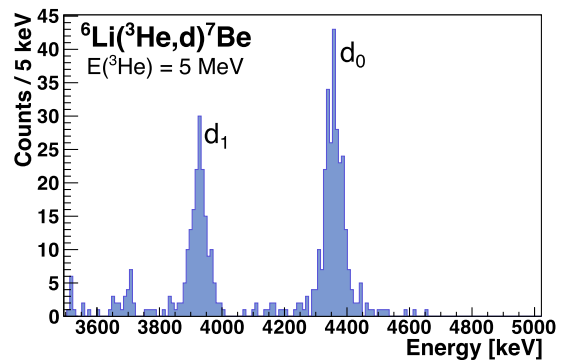


FIG. 1. 1D spectrum, deduced from signals of the 1st silicon ΔE -E telescope, positioned at the most forward configuration (15° in the laboratory), at $E_{lab.} = 5$ MeV beam energy. The peaks (marked with d_0 and d_1) used for the analysis are indicated, the integration was performed by fitting Gaussian functions. More details on the experiment can be found in [27].

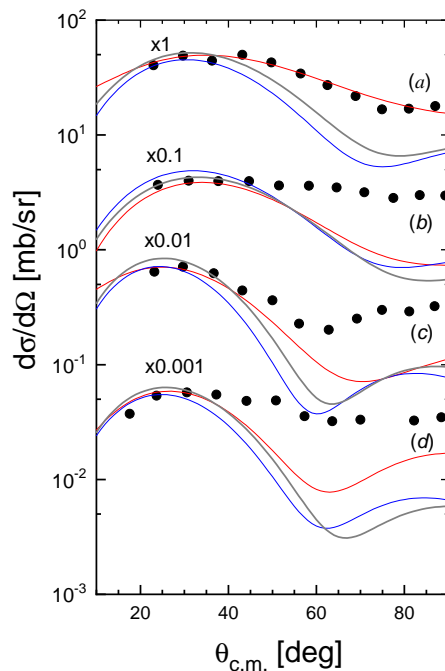


FIG. 2. Angular distributions of the ${}^6\text{Li}({}^3\text{He}, d){}^7\text{Be}$ differential cross section, at ${}^3\text{He}$ beam energies of $E_{lab.} = 3$ ((a) and (b)) and $E_{lab.} = 5$ ((c) and (d)) MeV, for the population of ${}^7\text{Be}$ in its ground ((a) and (c)) and first (0.429 MeV) excited ((b) and (d)) state. Error bars are generally smaller than the size of the points. The gray lines indicate the calculated angular distributions including coupled channels effects, for p -transfer off ${}^3\text{He}$. The red and blue curves are the same calculations, but with other optical potentials from [28, 29]. Data are taken from [27]. The exclusion of CCE (not shown) has a minor effect on the calculated angular distributions. For details see text.

(DCS) for the peripheral p -transfer reaction in the vicinity of the forward peak of the angular distribution can be written in the form:

$$\frac{d\sigma}{d\Omega} = \sum_{j_{6\text{Li}-p}} C_{6\text{Li}-p; j_{6\text{Li}-p}}^2 \times R_{p; j_{6\text{Li}-p}}^{(\text{DWBA})}(E_i, \theta; b_{d-p; j_{d-p}}, b_{6\text{Li}-p; j_{6\text{Li}-p}}), \quad (1)$$

and

$$R_{p; j_{6\text{Li}-p}}^{(\text{DWBA})}(E_i, \theta; b_{d-p; j_{d-p}}, b_{6\text{Li}-p; j_{6\text{Li}-p}}) = C_{d-p; j_{d-p}}^2 \frac{\sigma_{p; j_{6\text{Li}-p}}^{(\text{DWBA})}(E_i, \theta; b_{d-p; j_{d-p}}, b_{6\text{Li}-p; j_{6\text{Li}-p}})}{b_{d-p; j_{d-p}}^2 b_{6\text{Li}-p; j_{6\text{Li}-p}}^2} \quad (2)$$

where $l_{6\text{Li}-p}$ and $j_{6\text{Li}-p}$ are the orbital and total angular momenta of the transferred proton in the two-body ${}^7\text{Be} = {}^6\text{Li} + p$ system, and s -wave for ${}^3\text{He} \rightarrow d + p$ is taken into account (owing to its smallness, the d -wave ($l_{d-p} = 2$) contribution is ignored [31–33]). $l_{6\text{Li}-p} = 1$ and $j_{6\text{Li}-p} = 1/2$ and $3/2$ correspond to the ground and first excited (0.429 MeV) states of the ${}^7\text{Be}$ nucleus, respectively and $\sigma_{p; j_{6\text{Li}-p}}^{(\text{DWBA})}$ is the single-particle DWBA cross section [34]. Furthermore, $C_{6\text{Li}-p; j_{6\text{Li}-p}}^2$ and $C_{d-p; j_{d-p}}^2$ are the ANC's for ${}^6\text{Li} + p \rightarrow {}^7\text{Be}$ and $d + p \rightarrow {}^3\text{He}$, which determine the amplitudes of the tails of the radial ${}^7\text{Be}$ and ${}^3\text{He}$ wave functions in the ${}^6\text{Li} + p$ and $d + p$ channels [32]; $b_{d-p; j_{d-p}}, b_{6\text{Li}-p}$ are the single-particle ANC's for the shell-model wave functions for the two-body ${}^7\text{Be} = ({}^6\text{Li} + p)$ and ${}^3\text{He} = (d + p)$ bound states, which determine the amplitudes of their tails; E_i is the relative kinetic energy of the colliding particles and θ is the center-of-mass emission angle.

According to [35], the s -wave ANC value for $d + p \rightarrow {}^3\text{He}$ was taken equal to $3.9 \pm 0.06 \text{ fm}^{-1}$; this parameter is in good agreement with the experimentally determined one reported in [36]. As in [30, 37] the values of the $b_{d-p; j_{d-p}}$ parameters for $l_{d-p} = 0$ and $j_{d-p} = 1/2$ can be fixed by reproducing the corresponding ANC values entering the $R_{p; j_{6\text{Li}-p}}^{(\text{DWBA})}(E_i, \theta; b_{d-p; j_{d-p}}, b_{6\text{Li}-p; j_{6\text{Li}-p}})$ function calculated for the one-step proton transfer mechanism. In eqs. 1 and 2, the ANC's $C_{6\text{Li}-p; j_{6\text{Li}-p}}^2$ for ${}^6\text{Li} + p \rightarrow {}^7\text{Be}$ as well as the free model parameters $b_{6\text{Li}-p; j_{6\text{Li}-p}}$ are unknown.

Following eq. 1, the parametrization of the DCS makes it possible to determine the unknown ANC's. To this aim, for fixed values of $E_i, \theta, b_{d-p; j_{d-p}}$ the $R_{p; j_{6\text{Li}-p}}(b_{6\text{Li}-p}) = R_{p; j_{6\text{Li}-p}}^{(\text{DWBA})}(E_i, \theta; b_{d-p; j_{d-p}}, b_{6\text{Li}-p; j_{6\text{Li}-p}})$ function must not depend on variation of the free parameter $b_{6\text{Li}-p}$, where $b_{6\text{Li}-p} \equiv b_{6\text{Li}-p; j_{6\text{Li}-p}}$. The single-particle ANC's strongly depend on the geometric parameters (radius r_0 and diffuseness a) of the adopted Woods-Saxon potential, i.e., $b_{6\text{Li}-p} = b_{6\text{Li}-p}(r_0, a)$ [38]. Similarly to [38],

eq. 1 is then used to extract the experimental (“indirectly determined”) values of squared ANC's ($C_{6\text{Li}-p; j_{6\text{Li}-p}}^{\text{exp}}$)² for ${}^7\text{Be}$ ground and first excited states, and accordingly the $d\sigma/d\Omega$ in the left hand side of eq.1 is replaced by $d\sigma^{\text{exp}}/d\Omega$, measured in the forward hemisphere, for each of the experimental data points ($\theta = \theta^{\text{exp}}$) around the main peak of the angular distributions.

As discussed in [27], the one-step proton transfer is dominant in the forward hemisphere while one-step α particle exchange is the dominant contribution to the experimental differential cross section at large angles. However, due to the steep decrease of the calculated DCS approaching 90° , interference of the two mechanisms at small (forward) and large (backward) angular regions is negligible. To extract the ANC's for ${}^6\text{Li} + p \rightarrow {}^7\text{Be}$, the analysis of the angular distributions of the ${}^6\text{Li}({}^3\text{He}, d){}^7\text{Be}$ reaction measured at the ${}^3\text{He}$ beam energies of 3 and 5 MeV in the forward angular region was performed within the post form of the modified DWBA [30] using the LOLA code [34]. Following the prescription in [23], we focused on the main peak in the angular distribution, where the extraction of the ANC is most reliable since ANC can be determined from peripheral transfer reactions only. Thus, the analysis of the cross sections in the region of the main maximum of the angular distributions ($20^\circ \div 40^\circ$) gives the most precise information about the direct one-step mechanism of proton transfer.

First, eight sets of optical potentials, obtained from the global parametrization given in refs.[28, 29], in the input and output channels were used. The calculations show that the derived $R_{p; j_{6\text{Li}-p}}$ function is very sensitive to the sets of the optical potentials. Thanks to the properties of the ANC's discussed later in the manuscript, it is weakly dependent on the parameters of the potentials used in the data analysis, provided that the reaction process is pe-

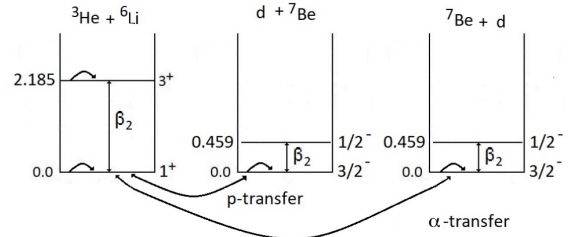


FIG. 3. The coupling schemes used in calculations of the DCSs for the proton transfer ${}^6\text{Li}({}^3\text{He}, d){}^7\text{Be}$ reaction and the α -particle exchange ${}^6\text{Li}({}^3\text{He}, {}^7\text{Be})d$ reaction by coupled channels method.

ripheral. In the further analysis we will take as reference the potential leading to the calculated angular distributions shown as gray lines in fig.2. Consistent results are obtained for the other potentials. The peripheral nature of the transfer reaction for each experimental data point (θ^{exp}) in the forward angular region was tested following the procedure described in ref.[38]. Namely, for the chosen optical potentials in the entrance and exit channels, the geometrical parameters r_0 and a of the Woods-Saxon potential (having the Thomas spin-orbit term) of the two-body ${}^7\text{Be} = ({}^6\text{Li} + p)$ bound state wave function were varied in the ranges $1.13 \leq r_0 \leq 1.40$ fm and $0.59 \leq a \leq 0.72$ fm. The depth of the potential well was adjusted to match the corresponding experimental binding energy for each (r_0, a) pair. It was found that the calculated $R_{p; j_{{}^6\text{Li}-p}}$ function is practically independent from varying the free parameters and changes within 2-3%.

By normalizing the calculated DCSs to the corresponding ($\theta = \theta^{\text{exp}}$) measured ones, the ‘‘indirectly determined’’ ANC values for ${}^6\text{Li} + p \rightarrow {}^7\text{Be}$ without and with taking into account the channels coupling effects (CCE) were derived. The squared ANCs values (C_p^2), their uncertainties for ${}^6\text{Li} + p \rightarrow {}^7\text{Be}$ ($E^* = 0.0$ MeV; $J^\pi = \frac{3}{2}^-$ and $E^* = 0.429$ MeV; $J^\pi = \frac{1}{2}^-$ for ground and first excited state of ${}^7\text{Be}$) obtained in the present work with and without the CCE contributions at $E_{3\text{He}} = 3.0$ and 5.0 MeV and their weighted mean values are listed in Table I. The values in square brackets are the experimental ($\Delta C_{\text{exp}; p}^2$) and theoretical ($\Delta C_{\text{th}; p}^2$) uncertainties, respectively. The experimental errors taken into account in the present work are twofold: $\Delta_{\text{exp}; p}^{(1)}$ is the relative uncertainty of each cross section value, including statistical and normalization uncertainties and $\Delta_{\text{exp}; 2}^{(2)}$ is the uncertainty of the ANC value of $d + p \rightarrow {}^3\text{He}$ as reported in ref.[35]. The theoretical uncertainty $\Delta_{\text{th}; p} = \Delta R_p^{(\text{DWBA})} / \bar{R}_p^{(\text{DWBA})}$ corresponds to the average squared uncertainty of the calculated R function values arising from the variation of the geometric parameters (r_0 and a) of the adopted Woods-Saxon potential, within the intervals mentioned above. $\bar{R}_p^{(\text{DWBA})}$ corresponds to the value of the $R_p^{(\text{DWBA})}$ function calculated for the standard values of r_0 and a ($r_0=1.25$ fm and $a=0.65$ fm). Finally, the total error $\Delta_{\text{tot}; p}$ is calculated summing in quadrature the total experimental and theoretical uncertainties.

The CCE contributions to the DWBA cross sections for each experimental point θ^{exp} from the forward peak region were determined using the FRESKO computational code [39]. Only one-step proton stripping ${}^6\text{Li}({}^3\text{He}, d){}^7\text{Be}$ was taken into account (similarly to ref.[27], where only α -transfer was considered). In these calculations, as shown in fig.3, the system of nine nucleons in the entrance channel, ${}^6\text{Li} + {}^3\text{He}$, was replaced by three subsystems: i) ${}^3\text{He} + {}^6\text{Li}$ (g.s., $J^\pi = 1^+$; $E^* = 2.185$ MeV, $J^\pi = 3^+$); ii) $d + {}^7\text{Be}$ (g.s., $J^\pi = 3/2^-$; $E^* = 0.429$

MeV, $J^\pi = 1/2^-$) and iii) ${}^7\text{Be}$ (g.s., $J^\pi = 3/2^-$; $E^* = 0.429$ MeV, $J^\pi = 1/2^-$) + d . All states of the subsystems ii) and iii) are coupled with the subsystem i) through proton (off ${}^3\text{He}$) and α -particle (off ${}^6\text{Li}$) transfers. Couplings between ground and excited states of nuclei ${}^6\text{Li}$ and ${}^7\text{Be}$ were calculated using the rotational model with the form factor $V_\lambda(r) = (\delta_\lambda/\sqrt{4\pi})dU(r)/dr$ for quadrupole transitions ($\lambda = 2$). Here, δ_λ is a deformation length, which is determined by $\delta_\lambda = \beta_\lambda R$, where R and β_λ are the nuclear radius and a deformation parameter, respectively.

The reorientation effects, determined by the matrix element $\langle E, J^\pi | V_2 | E, J^\pi \rangle$ [39], were also included in the coupling scheme. The deformation lengths δ_2 were taken equal to 3.0 fm for ${}^6\text{Li}$, and 2.0 for ${}^7\text{Be}$, which correspond to $\beta_2 = 0.73$ and $\beta_2 = 1.0$, respectively. These values are in a good agreement with the values obtained in refs. [38] and [40] from the analysis of the ${}^7\text{Be}(d, n){}^8\text{B}$ reaction and the $\alpha + {}^6,7\text{Li}$ scattering, respectively. Spectroscopic amplitudes for the ${}^3\text{He}$ and ${}^7\text{Be}$ nuclei in the $(d + p)$ and $({}^3\text{He} + \alpha)$ configurations, equal to 1.225 and 1.0913, were taken from the theoretical calculations performed in the framework of the translational invariant shell model [41]. The remaining spectroscopic amplitudes were determined by fitting the calculated angular distributions to the experimental data. For the $d - {}^6\text{Li}$ and $d - {}^3\text{He}$ core-core interactions in the proton transfer and α particle exchange mechanisms, the optical potentials were adopted for the entrance (${}^6\text{Li} + {}^3\text{He}$) channel and only the Coulomb component for the $d + {}^3\text{He}$ potential were used, respectively.

Calculations show that the CCE contribution to the ANCs enhances their values from 1.0% to 6.0% for ${}^6\text{Li} + p \rightarrow {}^7\text{Be}$ (g.s) and from 1.6% to 12% for ${}^6\text{Li} + p \rightarrow {}^7\text{Be}$ (0.429 MeV). The results of the calculations of the DCSs normalized to the corresponding forward peak of the angular distributions at $\theta = \theta_{\text{peak}}^{\text{exp}}$ (solid gray lines) and their comparison with the experimental data are displayed in fig.2. The weighted mean values of the square of the ANCs for ${}^6\text{Li} + p \rightarrow {}^7\text{Be}$ were found to be 4.81 ± 0.38 fm $^{-1}$ and 4.29 ± 0.27 fm $^{-1}$ for the ground and first excited states of ${}^7\text{Be}$, respectively, and correspond to their sum over $j_{{}^6\text{Li}-p}$ ($j_{{}^6\text{Li}-p} = 1/2$ and $3/2$). The different contributions to the total uncertainties are detailed in Table I. The overall uncertainties listed here correspond to the averaged squared errors, including both experimental errors in the $d\sigma^{\text{exp}}/d\Omega$ and the above-mentioned uncertainty of the ANC for $d + p \rightarrow {}^3\text{He}$ (since this is a common scaling factor, the error is propagated to the final uncertainty after taking the average) as well as the mentioned uncertainties in the $R_{p; j_{{}^6\text{Li}-p}}$ function.

III. THE INVERSE APPROACH: THEORETICAL ANALYSIS OF THE RECENT HIGH PRECISION ${}^6\text{Li}(p, \gamma){}^7\text{Be}$ DATA

To increase the accuracy of the astrophysical S-factor calculation, the ANCs for the ${}^6\text{Li} + p \rightarrow {}^7\text{Be}$ (g.s.) and

TABLE I. Summary of all uncertainties entering the evaluation of the ANC of the ${}^6\text{Li} + p \rightarrow {}^7\text{Be}$ system. $\Delta_{\text{exp};p}^{(1)}$, $\Delta_{\text{exp};p}^{(2)}$ and $\Delta_{\text{th};p}$ are calculated as described in the text. $\Delta_{\text{tot};p} = [(\Delta_{\text{exp};p}^{(1)})^2 + (\Delta_{\text{exp};p}^{(2)})^2 + \Delta_{\text{th};p}^2]^{1/2}$. Subscript p is neglected for ease of reading.

${}^6\text{Li} + p \rightarrow {}^7\text{Be}$												
$C_p^2 [\text{fm}^{-1}]$												
$E_{3\text{He}}$ [MeV]	E^* [MeV]	θ [deg]	without CCE			with CCE			$\Delta_{\text{exp}}^{(1)}$ [%]	$\Delta_{\text{exp}}^{(2)}$ [%]	Δ_{th} [%]	Δ_{tot} [%]
3.0	0.0	23.0	4.626±0.341	[0.080; 0.071; 0.323]	4.594±0.339	[0.079; 0.071; 0.322]	1.73	1.54	7.0	7.37		
		29.7	4.941±0.366	[0.091; 0.076; 0.346]	4.921±0.364	[0.090; 0.075; 0.344]	1.84	1.54	7.0	7.40		
		36.3	4.480±0.331	[0.081; 0.069; 0.314]	4.466±0.330	[0.081; 0.069; 0.313]	1.81	1.54	7.0	7.39		
5.0	0.0	23.2	4.505±0.346	[0.126; 0.069; 0.315]	4.761±0.367	[0.133; 0.073; 0.333]	2.79	1.54	7.0	7.69		
		29.7	4.946±0.366	[0.090; 0.076; 0.346]	5.243±0.388	[0.096; 0.081; 0.367]	1.83	1.54	7.1	7.39		
		36.7	5.374±0.397	[0.095; 0.083; 0.376]	5.691±0.420	[0.100; 0.087; 0.398]	1.76	1.54	7.1	7.38		
3.0	0.429	24.0	4.177±0.307	[0.068; 0.064; 0.292]	4.242±0.312	[0.069; 0.065; 0.297]	1.64	1.54	7.0	7.35		
		31.0	4.133±0.305	[0.072; 0.064; 0.289]	4.208±0.310	[0.074; 0.065; 0.294]	1.76	1.54	7.0	7.37		
		37.7	4.182±0.306	[0.063; 0.064; 0.293]	4.279±0.313	[0.065; 0.066; 0.299]	1.52	1.54	7.0	7.32		
5.0	0.429	17.6	3.964±0.313	[0.130; 0.061; 0.277]	4.317±0.340	[0.142; 0.066; 0.302]	3.29	1.54	7.0	7.88		
		23.7	4.750±0.376	[0.158; 0.073; 0.332]	5.277±0.418	[0.177; 0.081; 0.369]	3.36	1.54	7.0	7.91		
		30.6	5.231±0.402	[0.147; 0.081; 0.366]	5.864±0.451	[0.164; 0.090; 0.410]	2.80	1.54	7.0	7.69		
weighted mean values												
3.0+5.0	0.0		4.752±0.208	[0.123; 0.074; 0.151]	4.807±0.382	[0.247; 0.076; 0.282]		1.54	3.17	4.38		
3.0			4.665±0.241	[0.131; 0.072; 0.189]	4.643±0.239	[0.129; 0.072; 0.188]		1.54	4.05	5.16		
5.0			4.952±0.347	[0.229; 0.076; 0.250]	5.242±0.372	[0.246; 0.081; 0.267]		1.54	5.04	7.02		
3.0+5.0	0.429		4.199±0.172	[0.039; 0.068; 0.153]	4.295±0.274	[0.065; 0.072; 0.256]		1.54	3.65	4.10		
3.0			4.165±0.184	[0.039; 0.064; 0.168]	4.244±0.188	[0.040; 0.065; 0.171]		1.54	4.04	4.42		
5.0			4.555±0.542	[0.386; 0.071; 0.374]	5.023±0.662	[0.472; 0.079; 0.457]		1.54	8.21	11.91		

${}^6\text{Li} + p \rightarrow {}^7\text{Be}(0.429 \text{ MeV})$ channels, were derived from the experimental total astrophysical S-factor and the branching ratios of ref. [17], within the modified two body potential method (MTBPM) [26]. To this purpose, we have applied the MTBPM to the analysis of the ${}^6\text{Li}(p,\gamma){}^7\text{Be}$ S-factor [17], using the experimental branching ratio to separate the total experimental S-factor into two contributions corresponding to the ground and first excited states of the residual ${}^7\text{Be}$ nucleus for all experimental points of energy E , as described in the following sections.

A. Basic formulas of MTBPM

According to the MTBPM (see also [24, 42, 43]), the astrophysical S factors $S_{l_f j_f}(E)$ [or $S_{aA}(E)$] of the direct radiative capture $A(a,\gamma)B$ reaction has the form

$$S_{l_f j_f}(E) = C_{l_f j_f}^2 R_{l_f j_f}(E, b_{l_f j_f}). \quad (3)$$

Here, $C_{l_f j_f}^2$ (or $C_{A-a; j_f}^2$) is the ANC for $a + A \rightarrow B$. $R_{l_f j_f}$ is given by:

$$R_{l_f j_f} = \frac{S_{l_f j_f}^{sp}(E)}{b_{l_f j_f}^2}, \quad (4)$$

where $S_{l_f j_f}^{sp}(E)$ is the single particle (sp) calculated astrophysical S factor, $b_{l_f j_f}$ is the single particle ANC, which determines the amplitude of the tail of the radial component of the bound $A + a$ shell-model wave function of B , calculated using the Schrödinger equation with a suitable Woods-Saxon potential; $l_f(j_f)$ is a relative orbital (total) angular momentum of A and a particles in nucleus $B(a + A)$. By enforcing the following additional requirements [26]

$$R_{l_f j_f}(E, b_{l_f j_f}) = f(E) \quad (5)$$

and

$$C_{l_f j_f}^2 = \frac{S_{l_f j_f}(E)}{R_{l_f j_f}(E, b_{l_f j_f})} = \text{const} \quad (6)$$

for each energy $E = E_i$ ($i = 1, 2, \dots, N$, N being the number of the experimental points), and by analysing the experimental phase shifts for the $a + A$ scattering, it is possible to derive the “indirectly determined” (experimental) value of the ANC ($C_{l_f j_f}^{exp}$)² and its uncertainty by model-independent way. To obtain the value of the ANC, the directly measured astrophysical S factors $S_{aA}^{exp}(E)$ are used instead of $S_{l_f j_f}(E)$ in Eq.6, i.e.

$$(C_{l_f j_f}^{exp})^2 = \frac{S_{aA}^{exp}(E)}{R_{l_f j_f}(E, b_{l_f j_f})}. \quad (7)$$

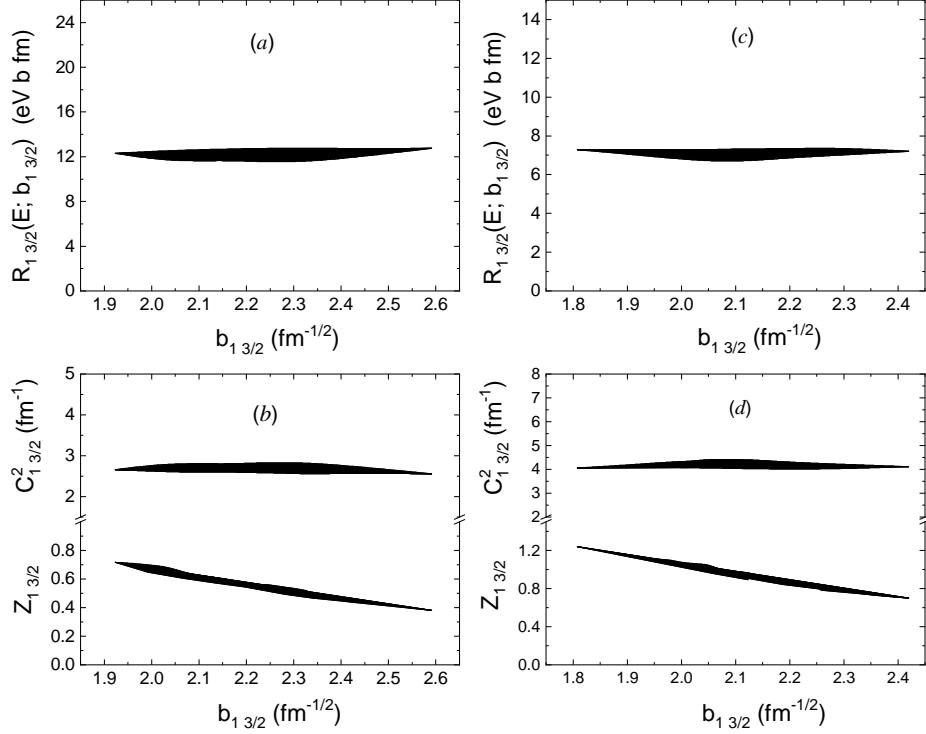


FIG. 4. The dependence of $R_{l_f j_f}(E, b_{l_f j_f})$ [panels (a) and (c)] as a function of the single-particle ANC $b_{l_f j_f}$ for the ${}^6\text{Li}(p, \gamma){}^7\text{Be}(\text{g.s.})$ [$l_f = 1$ and $j_f = 3/2$] (a) and for the ${}^6\text{Li}(p, \gamma){}^7\text{Be}(0.429 \text{ MeV})$ [$l_f = 1$ and $j_f = 3/2$] (c) reactions at $E = 60 \text{ keV}$ (minimum measured energy in [17]). The dependence of the ANCs $C_{l_f j_f}^2$ [upper bands in panels (b) and (d)] and of the spectroscopic factors $Z_{l_f j_f}$ [lower bands in panels (b) and (d)] on the single particle ANCs $b_{l_f j_f}$ for the ${}^6\text{Li}(p, \gamma){}^7\text{Be}(\text{g.s.})$ [left column, $l_f = 1$ and $j_f = 3/2$] (b) and for the ${}^6\text{Li}(p, \gamma){}^7\text{Be}(0.429 \text{ MeV})$ [right column, $l_f = 1$ and $j_f = 3/2$] (d) reactions at $E = 60 \text{ keV}$. The width of the bands corresponds to the variation of the geometrical parameters of the adopted Woods-Saxon potential.

B. Extraction of the ANCs from the recent direct experimental data

Let us write $l_f(j_f)$ for the relative orbital (total) angular momentum of ${}^6\text{Li}$ and proton in ${}^7\text{Be}({}^6\text{Li}+p)$. For the ${}^6\text{Li}(p, \gamma){}^7\text{Be}$ reaction populating the ground ($E^* = 0.0$; $J^\pi = 3/2^-$) and first excited ($E^* = 0.429 \text{ MeV}$; $J^\pi = 1/2^-$) states of ${}^7\text{Be}$, the values j_f are taken to be $1/2$ and $3/2$, the value of l_f is taken to be equal to 1. The ANC ($C_{l_f j_f}^{\text{exp}})^2$ values for ${}^6\text{Li}(p, \gamma){}^7\text{Be}(0 \text{ MeV})$ and ${}^6\text{Li}(p, \gamma){}^7\text{Be}(0.429 \text{ MeV})$ were obtained by applying the relations (3)-(7).

To this purpose, we vary the geometric parameters of the adopted Woods-Saxon potential in the physically acceptable ranges $1.13 \leq r_0 \leq 1.40$ and $0.59 \leq a \leq 0.72 \text{ fm}$ with respect to their standard values ($r_0 = 1.25 \text{ fm}$ and $a = 0.65 \text{ fm}$), and adjust the depth to fit the binding energies. Such variation of the r_0 and a parameters changes the single particle ANC with $j_f = 3/2$ in the ranges $1.92 \leq b_{1,3/2} \leq 2.59 \text{ fm}^{-1/2}$ for the ground state and

$1.81 \leq b_{1,3/2} \leq 2.42 \text{ fm}^{-1/2}$ for the first excited state of ${}^7\text{Be}$. The difference between values of the single-particle asymptotic normalization coefficients $b_{1,1/2}$ and $b_{1,3/2}$ at both considered proton bound states of the ${}^7\text{Be}$ nucleus is small (less than 0.3%).

In fig.4(a) and 4(c) the dependence of the $R_{1,3/2}(E, b_{1,3/2})$ function on the single-particle ANC $b_{1,3/2}$ at $E = 60 \text{ keV}$ for ${}^7\text{Be}$ ground and first excited states is presented (minimum measured energy in [17]). The width of the bands is the result of the weak “residual” (r_0, a) dependence of $R_{1,3/2}(E, b_{1,3/2})$ on the parameters r_0 and a (up to $\pm 3\%$). For example, the arithmetic averaged values of $R_{1,3/2}(E, b_{1,3/2})$ in the intervals of $b_{1,3/2}$ mentioned above are equal to 12.21 ± 0.34 and $7.06 \pm 0.17 \text{ eV b fm}$ at $E = 60 \text{ keV}$ for ${}^7\text{Be}$ ground and first excited states, respectively. Variation of r_0 and a changes $R_{1,3/2}(E, b_{1,3/2})$ in the ranges $11.54 \leq R_{1,3/2}(E, b_{1,3/2}) \leq 12.80 \text{ eV b fm}$ for the ground state and $6.67 \leq R_{1,3/2}(E, b_{1,3/2}) \leq 7.37 \text{ eV b fm}$ for ${}^7\text{Be}$ first excited state. The same dependence is also observed for $j_f = 1/2$.

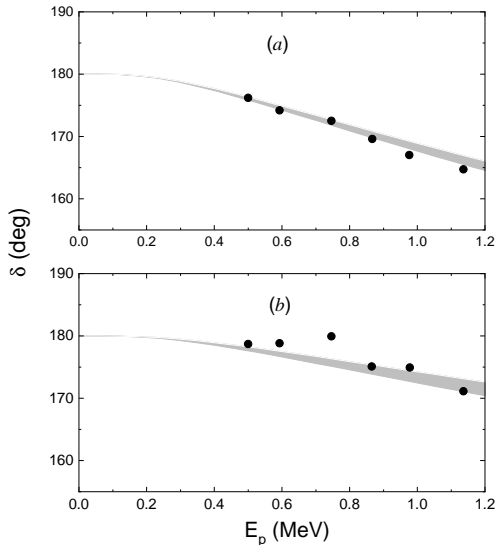


FIG. 5. Energy dependence of the p - ${}^6\text{Li}$ elastic-scattering phase shifts for the ${}^2S_{1/2}$ and the ${}^4S_{3/2}$ partial waves. The experimental data are taken from ref.[44] (the error bar is smaller than the point size).

For $E = 60$ keV the dependence of the ANC $C_{l_f j_f}^2$ and of the spectroscopic factor $Z_{l_f j_f}$ on the single-particle ANC $b_{l_f j_f}$ with $j_f = 3/2$ for ground and first excited states of ${}^7\text{Be}$ are presented in fig.4 (b) and 4(d), respectively. Variation of r_0 and a changes $C_{1 j_f}^2$ ($j_f = 1/2$ and $j_f = 3/2$) in the ranges $2.03 \leq C_{1 1/2}^2 \leq 2.25 \text{ fm}^{-1}$ and $2.55 \leq C_{1 3/2}^2 \leq 2.83 \text{ fm}^{-1}$ for the ground state, $0.512 \leq C_{1 1/2}^2 \leq 0.56 \text{ fm}^{-1}$ and $4.00 \leq C_{1 3/2}^2 \leq 4.42 \text{ fm}^{-1}$ for the first excited state of ${}^7\text{Be}$ nucleus at $E = 60$ keV. The calculated values of $C_{1 3/2}^2$ and $C_{1 1/2}^2$ are weakly depending on the values of the single-particle asymptotic normalization coefficients. Instead, changing r_0 and a in the same range causes a variation of the spectroscopic factor $Z_{1 j_f}$ ($j_f = 1/2$ and $j_f = 3/2$) in the ranges $0.30 \leq Z_{1 1/2} \leq 0.57$ and $0.38 \leq Z_{1 3/2} \leq 0.71$ for the ground state, $0.09 \leq Z_{1 1/2} \leq 0.16$ and $0.70 \leq Z_{1 3/2} \leq 1.23$ for the first excited state of ${}^7\text{Be}$ at $E = 60$ keV.

Therefore, the values of the spectroscopic factors $Z_{1 3/2}$ and $Z_{1 1/2}$ corresponding to the ground and first excited states strongly depend on the single-particle ANCs. Similar dependence is also observed for the other experimental energies. On the other hand, such weak dependence of the ANCs on the $b_{l_f j_f}$ parameters makes us confident on the peripheral character of the ${}^6\text{Li}(p, \gamma){}^7\text{Be}$ reaction. This is a pivotal test for the further analysis, as already done in [24].

To cross check the validity of the present approach, the phase shifts of ${}^6\text{Li}-p$ elastic scattering are calculated by varying the parameters r_0 and a of the adopted Woods-

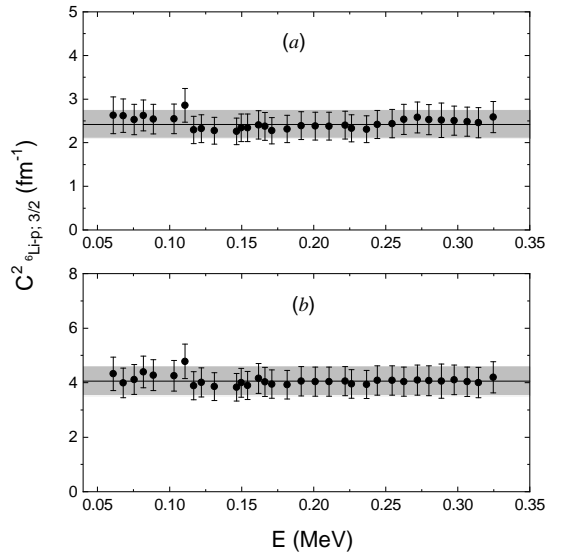


FIG. 6. The values of the ANCs, $C_{1 3/2}^2$ for ${}^6\text{Li}+p \rightarrow {}^7\text{Be}(\text{g.s.})$ in panel (a) and for ${}^6\text{Li}+p \rightarrow {}^7\text{Be}(0.429\text{MeV})$ in panel (b) for each experimental energy point. The solid lines are the present results weighted means. The width of each band is the corresponding weighted uncertainty.

Saxon potential in the same intervals. As an illustration, the results of the calculations corresponding to the ${}^2S_{1/2}$ and ${}^4S_{3/2}$ waves only are presented in fig.5. The band width in fig.5 corresponds to the change of the calculated values of phase shifts with respect to the variation of the r_0 and a parameters. As seen from fig.5, the experimental phase shifts [44] are fairly well reproduced within the uncertainty of about $\pm 2.5\%$. The same results are also obtained for the ${}^2P_{1/2}$ waves.

Finally, for each of the thirty three experimental points of energy E , the values of the ANCs $C_{1 j_f}^{exp}$ ($j_f = 1/2$ and $j_f = 3/2$) for ${}^6\text{Li}(p, \gamma){}^7\text{Be}(\text{g.s.})$ and $C_{1 j_f}^{exp}$ ($j_f = 1/2$ and $j_f = 3/2$) for ${}^6\text{Li}(p, \gamma){}^7\text{Be}(0.429 \text{ MeV})$ are obtained by using the corresponding experimental astrophysical S-factor from [17] in Eq.(6) in the place of $S_{1 j_f}(E)$, and by using the central values of $R_{1 j_f}(E, b_{l_f j_f})$, corresponding to the standard values of the parameters r_0 and a of the adopted Woods-Saxon potential ($r_0 = 1.25$ and $a = 0.65$ fm). To determine the values of the ANCs $C_{1 1/2}^2$ and $C_{1 3/2}^2$ we use the assumption $C_{1 1/2}^2/C_{1 3/2}^2 \simeq Z_{1 1/2}/Z_{1 3/2}$, where the $Z_{1 1/2}$ and $Z_{1 3/2}$ spectroscopic factors are the theoretical values found in [45]. Here we used $Z_{1 3/2} = 0.54$ and $Z_{1 1/2} = 0.11$ for the ground state and $Z_{1 3/2} = 0.86$ and $Z_{1 1/2} = 0.11$ for the excited state of ${}^7\text{Be}$ (see [46] and references therein).

The calculated ANCs for all the experimental energy points are shown in fig.6 as a function of the c.m. energy E . In the same figure, the solid line and the band are used to mark the weighted means of the ANC values

TABLE II. The weighted means of the ANC values $(C^{exp})^2$ for ${}^6\text{Li} + p \rightarrow {}^7\text{Be}$. Here, numbers in square brackets are statistical, theoretical and experimental systematic uncertainties, respectively. For comparison, in the last column the ANCs from the ${}^6\text{Li}({}^3\text{He}, d){}^7\text{Be}$ transfer reactions (sec.II B) are shown.

E^* [MeV]	$C_{11/2}^2$ [fm $^{-1}$]	$C_{13/2}^2$ [fm $^{-1}$]	$C_{11/2}^2 + C_{13/2}^2$ [fm $^{-1}$]	$C_{11/2}^2 + C_{13/2}^2$ [fm $^{-1}$]
0.0	1.926 ± 0.256 [0.015; 0.018; 0.255]	2.419 ± 0.320 [0.018; 0.023; 0.319]	4.345 ± 0.576 [0.033; 0.041; 0.574]	4.81 ± 0.38 fm $^{-1}$
0.429	0.519 ± 0.067 [0.003; 0.004; 0.067]	4.052 ± 0.528 [0.024; 0.030; 0.527]	4.571 ± 0.595 [0.027; 0.033; 0.594]	4.29 ± 0.27 fm $^{-1}$

and the propagated uncertainty, respectively. The values of the weighted means for the ANC values for ${}^7\text{Be}$ ground and first excited states obtained from all experimental data in [17] are equal to $(C_{11/2+13/2}^{exp})^2 = 4.345 \pm 0.576$ [0.033; 0.041; 0.574] fm $^{-1}$ and $(C_{11/2+13/2}^{exp})^2 = 4.571 \pm 0.595$ [0.027; 0.033; 0.594] fm $^{-1}$, respectively. Here, numbers in square brackets are the statistical errors, the theoretical uncertainties, and the contribution due to the experimental systematic error affecting data in [17], respectively. They include the total experimental errors in the corresponding experimental astrophysical S_{61} factor and the uncertainty on $R_{1jf}(E, b_{1jf})$ (see fig.4 (a) and (c)). It is important noting that, since the systematic error of about 13% affects all the experimental data [17], this component of the uncertainty has not been used in the weighted average of the ANCs, but added in quadrature to the resulting ANCs. The weighted means of the ANC values for ${}^6\text{Li} + p \rightarrow {}^7\text{Be}(\text{g.s.})$ and ${}^6\text{Li} + p \rightarrow {}^7\text{Be}(0.429\text{MeV})$ are also given in tab.II, together with the uncertainties evaluated as discussed.

The above weighted mean values of ANCs are in excellent agreement with the values of ANCs (4.81 ± 0.38 fm $^{-1}$ for the ground and 4.29 ± 0.27 fm $^{-1}$ for the first excited state of ${}^7\text{Be}$) extracted from the analysis of the ${}^6\text{Li}({}^3\text{He}, d){}^7\text{Be}$ transfer reaction at $E_{3\text{He}} = 3$ and 5 MeV, confirming the accuracy of our analysis. For ease of comparison, such values of the ANCs are also shown in Table II (rightmost column) along with the ANCs deduced from the S-factor in [17].

IV. RESULTS AND CONSEQUENCES

The weighted means of the ANCs from the analysis of the ${}^6\text{Li}({}^3\text{He}, d){}^7\text{Be}$ transfer reaction were used to calculate the total astrophysical S-factor for the ${}^6\text{Li}(p, \gamma){}^7\text{Be}$ reaction at low energies E , including $E = 0$. The calculations were performed within the modified two-body potential method [26].

The main contributions to the radiative capture reaction ${}^6\text{Li}(p, \gamma){}^7\text{Be}$ astrophysical S-factor comes from the $E1$ transition. The contributions of $M1$ and $E2$ are negligible in the aforementioned energy region and below, including solar energy. They vary from about 0.4% up to about 1% as the energy increases. Therefore, they will be neglected in the following calculations.

The results of the calculations and the comparison with

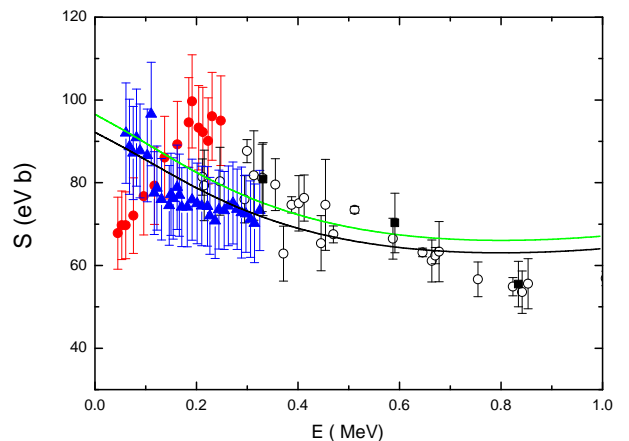


FIG. 7. The experimental and calculated astrophysical S-factor for the radiative-capture ${}^6\text{Li}(p, \gamma){}^7\text{Be}$ reaction. Solid green and black lines represent the results of this work for the direct component of the astrophysical S factor, obtained using the weighted average ANC values from the near-barrier proton transfer ${}^6\text{Li}({}^3\text{He}, d){}^7\text{Be}$ reaction at $E_{3\text{He}}=3$ and 5 MeV and the one from the analysis of ${}^6\text{Li}(p, \gamma){}^7\text{Be}$ reaction [17], respectively. Blue solid triangles represent the bare-nucleus astrophysical factor from ref.[17] (including systematic error), red filled circles are the experimental astrophysical factor published in [15], empty circles are taken from [14] and black solid squares from [31].

the literature data are shown in fig.7 as a solid green line. At $E=0$, the indirect $S_{61}^{(\text{DC})}(E)$ (DC stands for direct capture) equals 65.781 ± 5.227 [3.380; 1.040; 3.859] eV·b and 30.675 ± 1.957 [0.464; 0.514; 1.828] eV·b for the ground and the first excited states of ${}^7\text{Be}$, respectively, leading to a total S-factor of 96.5 ± 5.7 eV·b. This value is in excellent agreement with the extrapolated S-factor to zero energy ($S(0) = 95 \pm 9$ eV·b) of [17], with an uncertainty 1.6 times lower. It is worth noting that our approach is entirely independent from their direct measurement; possible systematic errors are independent and of radically different nature than the ones affecting the LUNA measurement [17], thus supplying an invaluable validation of their results. Furthermore, the indirect result does not support the occurrence of the 200 keV resonance claimed in [15].

We also calculated the astrophysical factor of the

TABLE III. The calculated values of S_{61} at energies $E = 0, 15.1$ keV and 25 keV using the weighted means of the ANC values $(C^{exp})^2$ in tab.II. Also here figures in square brackets are statistical, theoretical, and experimental systematic uncertainties, respectively.

E^* [MeV]	$S_{61}(0.0 \text{ keV})$ [eV b]	$S_{61}(15.1 \text{ keV})$ [eV b]	$S_{61}(25 \text{ keV})$ [eV b]
0.0	59.46 ± 7.88 [0.45; 0.56; 7.85]	58.89 ± 7.80 [0.44; 0.55; 7.78]	58.48 ± 7.75 [0.44; 0.55; 7.72]
0.429	32.64 ± 4.25 [0.19; 0.24; 4.24]	32.32 ± 4.21 [0.19; 0.24; 4.20]	32.09 ± 4.18 [0.18; 0.23; 4.17]
total	92.10 ± 12.13 [0.64; 0.80; 12.09]	91.21 ± 12.01 [0.63; 0.79; 11.98]	90.57 ± 11.93 [0.62; 0.78; 11.89]

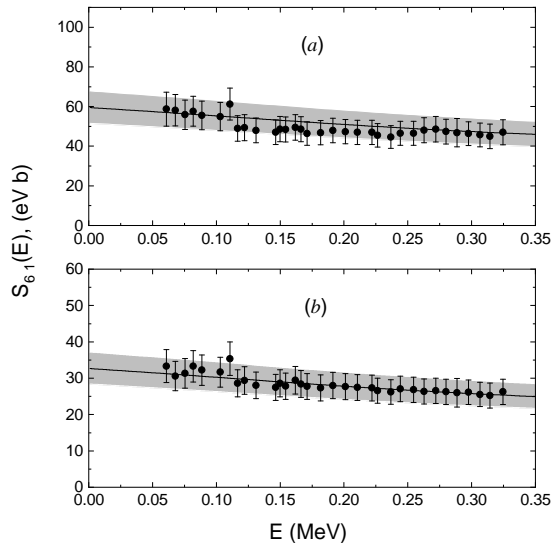


FIG. 8. In (a) [$E^* = 0$ MeV] and (b) [$E^* = 0.429$ MeV] the solid lines are the calculated astrophysical factors within the MTBPM. The solid circles are the experimental astrophysical S factor $S_{61}^{exp}(E)$ for the ground (a) and the first excited (b) states of ${}^7\text{Be}$ from ref. [17]. The width of the bands corresponds to the uncertainty introduced by the variation of the geometrical parameters of the adopted Woods-Saxon potential (theoretical error), summed to the experimental errors, made up of two contributions: statistic and systematic uncertainties. The latter is the dominant contribution (see text for details).

${}^6\text{Li}(p, \gamma){}^7\text{Be}$ reaction within the MTBPM [26], using the values of ANCs obtained from the analysis of the experimental astrophysical S-factors of the radiative capture ${}^6\text{Li}(p, \gamma){}^7\text{Be}$ reaction [17]. In detail, the weighted average values of the ANCs were used to calculate the astrophysical factors corresponding to the ground and first excited states of ${}^7\text{Be}$. These calculated astrophysical factors are shown in fig.8 (a) and (b), respectively, while their sum leading to the total astrophysical factor is shown as a solid black line in fig.7. The values of S_{61} at different energies, calculated by using the values of ANCs obtained from the ${}^6\text{Li}(p, \gamma){}^7\text{Be}$ reaction, are given in tab. III.

In particular, for $S_{61}(E)$, the following values were found: 92 ± 12 eV b for $E = 0$ and 91 ± 12 eV b for

$E = 15.1$ eV (the energy of the Gamow peak). Note that the values of $S_{61}(0)$ and $S_{61}(15.1 \text{ keV})$ differ from those $S_{61}(0) = 66.0 \pm 9.9$ eV b and $S_{61}(15.1 \text{ keV}) = 75.0 \pm 11.3$ eV b [47], which were obtained within the framework of the standard two-body potential model with the assumption that the spectroscopic factors (SF) are equal to 1. In fact, as can be seen from [46], the above SFs cannot be determined unambiguously, and their values should not be assumed to be equal to 1, a priori. The values of the total astrophysical factor at $E = 0$ calculated by using the ANC obtained from the ${}^6\text{Li}(p, \gamma){}^7\text{Be}$ reaction is in excellent agreement with the values calculated using the ANCs determined from the near-barrier proton transfer ${}^6\text{Li}({}^3\text{He}, d){}^7\text{Be}$ reaction at $E_{3\text{He}} = 3$ and 5 MeV. The obtained 92 ± 12 eV b value is also in good agreement with the extrapolated S-factor to zero energy 95 ± 9 eV b in [17]. The comparison with the results of ref.[6] shows that the $S_{61}(0)$ value obtained in this work is in good agreement with the “bare-nucleus” calculation (about 95 eV b) in [6].

Moreover, the good agreement between the present-work astrophysical factor and the electron-screening-corrected S_{61} of [17] shows that either the electron screening potential value from the adiabatic approximation is a good estimate of it or the uncertainty affecting direct data is still not good enough to provide an accurate determination of this parameter.

ACKNOWLEDGMENTS

The authors are deeply indebted to late R. Yarmukhamedov for his enthusiasm and guidance in the preparation of this work. This work was supported by INFN (Istituto Nazionale di Fisica Nucleare), by NK-FIH (NN128072 and FK134845), and by the New National Excellence Program of the Ministry of Human Capacities of Hungary (ÚNKP-20-5-DE-2 and ÚNKP-20-5-DE-297), and supported in part by the National Science Foundation, Grant No. PHY-1712953 (USA), and by the University of Catania (Finanziamenti di linea 2 and Starting grant 2020). G. G. Kiss and T. Szücs acknowledge the support from the János Bolyai research fellowship of the Hungarian Academy of Sciences. R. Yarmukhamedov and K.I. Tursunmakhatov acknowledge the support from the Academy of Sciences of the Republic of Uzbekistan. J. Mrázek and G. D’Agata acknowl-

edge the support from MEYS Czech Republic under the project EF16_013/0001679. A.M. Mukhamedzhanov acknowledges support from the U.S. DOE Grant No. DE-

FG02-93ER40773 and NNSA Grant No. DENA0003841. The authors acknowledge the support of prof. M. G. Grimaldi and of the technical staff of the DFA.

-
- [1] S. E. Woosley, D. H. Hartmann, R. D. Hoffman, and W. C. Haxton, The nu -Process, *The Astrophysical Journal* **356**, 272 (1990).
- [2] C. E. Rolfs and W. S. Rodney, *Cauldrons in the cosmos: nuclear astrophysics* (University of Chicago Press, Chicago, USA, 1988).
- [3] B. D. Fields, K. A. Olive, T.-H. Yeh, and C. Young, Big-Bang Nucleosynthesis after Planck, *J. Cosmol. Astropart. Phys.* **2020** (3), 010, arXiv:1912.01132 [astro-ph.CO].
- [4] D. Clayton, *Handbook of Isotopes in the Cosmos* (Cambridge University Press, Cambridge, UK, 2003).
- [5] F. Spite and M. Spite, Abundance of lithium in unevolved stars and old disk stars : Interpretation and consequences., *Astronomy and Astrophysics* **115**, 357 (1982).
- [6] A. Gnech and L. E. Marcucci, Theoretical calculation of the p - ${}^6\text{Li}$ radiative capture reaction, *Nucl. Phys. A* **987**, 1 (2019), arXiv:1902.05881 [nucl-th].
- [7] D. N. Schramm and R. V. Wagoner, Element production in the early universe., *Annual Review of Nuclear and Particle Science* **27**, 37 (1977).
- [8] K. M. Nollett, M. Lemoine, and D. N. Schramm, Nuclear reaction rates and primordial ${}^6\text{Li}$, *Phys. Rev. C* **56**, 1144 (1997), arXiv:astro-ph/9612197 [astro-ph].
- [9] E. Vangioni-Flam, M. Cassé, and J. Audouze, Lithium-beryllium-boron: origin and evolution, *Physics Reports* **333**, 365 (2000), arXiv:astro-ph/9907171 [astro-ph].
- [10] I. J. Sackmann and A. I. Boothroyd, Creation of ${}^7\text{Li}$ and Destruction of ${}^3\text{He}$, ${}^9\text{Be}$, ${}^{10}\text{B}$, and ${}^{11}\text{B}$ in Low-Mass Red Giants, Due to Deep Circulation, *The Astrophysical Journal* **510**, 217 (1999).
- [11] H. J. Assenbaum, K. Langanke, and C. Rolfs, Effects of electron screening on low-energy fusion cross sections., *Zeitschrift fur Physik A Hadrons and Nuclei* **327**, 461 (1987).
- [12] R. G. Pizzone, R. Spartá, C. A. Bertulani, C. Spitaleri, M. La Cognata, J. Lalmansingh, L. Lamia, A. Mukhamedzhanov, and A. Tumino, Big Bang Nucleosynthesis Revisited via Trojan Horse Method Measurements, *Astrophys. J.* **786**, 112 (2014), arXiv:1403.4909 [nucl-ex].
- [13] C. Angulo, M. Arnould, M. Rayet, P. Descouvemont, D. Baye, C. Leclercq-Willain, A. Coc, S. Barhoumi, P. Aguer, C. Rolfs, R. Kunz, J. W. Hammer, A. Mayer, T. Paradellis, S. Kossionides, C. Chronidou, K. Spyrou, S. degl'Innocenti, G. Fiorentini, B. Ricci, S. Zavatarelli, C. Providencia, H. Wolters, J. Soares, C. Grama, J. Rahighi, A. Shotton, and M. Laméhi Rachti, A compilation of charged-particle induced thermonuclear reaction rates, *Nucl. Phys. A* **656**, 3 (1999).
- [14] Z. E. Switkowski, J. C. P. Heggie, D. L. Kennedy, D. G. Sargood, F. C. Barker, and R. H. Spear, Cross section of the reaction ${}^6\text{Li}(p, \gamma) {}^7\text{Be}$, *Nuclear Physics A* **331**, 50 (1979).
- [15] J. J. He, S. Z. Chen, C. E. Rolfs, S. W. Xu, J. Hu, X. W. Ma, M. Wiescher, R. J. deBoer, T. Kajino, M. Kusakabe, L. Y. Zhang, S. Q. Hou, X. Q. Yu, N. T. Zhang, G. Lian, Y. H. Zhang, X. H. Zhou, H. S. Xu, G. Q. Xiao, and W. L. Zhan, A drop in the ${}^6\text{Li}(p, \gamma) {}^7\text{Be}$ reaction at low energies, *Physics Letters B* **725**, 287 (2013).
- [16] T. Szücs, G. G. Kiss, G. Gyürky, Z. Halász, T. N. Szegedi, and Z. Fülöp, Cross section of ${}^3\text{He}(\alpha, \gamma) {}^7\text{Be}$ around the ${}^7\text{Be}$ proton separation threshold, *Phys. Rev. C* **99**, 055804 (2019), arXiv:1905.01711 [nucl-ex].
- [17] D. Piatti, T. Chillery, R. Depalo, M. Aliotta, D. Bemmerer, A. Best, A. Boeltzig, C. Brogini, C. G. Bruno, A. Cacioli, F. Cavanna, G. F. Ciani, P. Corvisiero, L. Csedreki, T. Davinson, A. Di Leva, Z. Elekes, F. Ferraro, E. M. Fiore, A. Formicola, Z. Fülöp, G. Gervino, A. Gnech, A. Guglielmetti, C. Gustavino, G. Gyürky, G. Imbriani, M. Junker, I. Kochanek, M. Lugaro, L. E. Marcucci, P. Marigo, E. Masha, R. Menegazzo, V. Mossa, F. R. Pantaleo, V. Patichio, R. Perrino, P. Prati, L. Schiavulli, K. Stöckel, O. Straniero, T. Szücs, M. P. Takács, and S. Zavatarelli (LUNA Collaboration), Underground experimental study finds no evidence of low-energy resonance in the ${}^6\text{Li}(p, \gamma) {}^7\text{Be}$ reaction, *Phys. Rev. C* **102**, 052802 (2020).
- [18] L. Lamia, C. Spitaleri, R. G. Pizzone, E. Tognelli, A. Tumino, S. Degl'Innocenti, P. G. Prada Moroni, M. La Cognata, L. Pappalardo, and M. L. Sergi, An Updated ${}^6\text{Li}(p, \alpha) {}^3\text{He}$ Reaction Rate at Astrophysical Energies with the Trojan Horse Method, *The Astrophysical Journal* **768**, 65 (2013).
- [19] Y. Xu, K. Takahashi, S. Goriely, M. Arnould, M. Ohta, and H. Utsunomiya, NACRE II: an update of the NACRE compilation of charged-particle-induced thermonuclear reaction rates for nuclei with mass number $A < 16$, *Nucl. Phys. A* **918**, 61 (2013), arXiv:1310.7099 [nucl-th].
- [20] G. X. Dong, N. Michel, K. Fosse, M. Płoszajczak, Y. Jaganathen, and R. M. I. Betan, Gamow shell model description of radiative capture reactions ${}^6\text{Li}(p, \gamma) {}^7\text{Be}$ and ${}^6\text{Li}(n, \gamma) {}^7\text{Li}$, *Journal of Physics G Nuclear Physics* **44**, 045201 (2017), arXiv:1601.06660 [nucl-th].
- [21] K. Arai, D. Baye, and P. Descouvemont, *Nucl. Phys. A* **699**, 963 (2002).
- [22] Z.-H. Li, E.-T. Li, J. Su, Y.-J. Li, Y.-B. Wang, S.-Q. Yan, B. Guo, D. Nan, and W.-P. Liu, New determination of the ${}^7\text{Be}$ ground state spectroscopic factor and the ${}^6\text{Li}(p, \gamma) {}^7\text{Be}$ astrophysical $S(E)$ factors, *Chinese Physics C* **42**, 065001 (2018).
- [23] R. E. Tribble, C. A. Bertulani, M. La Cognata, A. M. Mukhamedzhanov, and C. Spitaleri, Indirect techniques in nuclear astrophysics: a review, *Reports on Progress in Physics* **77**, 106901 (2014).
- [24] Q. I. Tursunmahatov and R. Yarmukhamedov, Determination of the ${}^3\text{He}+\alpha \rightarrow {}^7\text{Be}$ asymptotic normalization coefficients, the nuclear vertex constants, and their application for the extrapolation of the ${}^3\text{He}(\alpha, \gamma) {}^7\text{Be}$ astrophysical S factors to the solar energy region, *Physical Review C* **85**, 045807 (2012), arXiv:0905.2026 [nucl-th].
- [25] H. M. Xu, C. A. Gagliardi, R. E. Tribble, A. M.

- Mukhamedzhanov, and N. K. Timofeyuk, Overall normalization of the astrophysical S factor and the nuclear vertex constant for ${}^7\text{Be}(p,\gamma){}^8\text{B}$ reactions, *Physical Review Letters* **73**, 2027 (1994).
- [26] S. B. Igamov and R. Yarmukhamedov, Modified two-body potential approach to the peripheral direct capture astrophysical $a+A\rightarrow B+\gamma$ reaction and asymptotic normalization coefficients, *Nuclear Physics A* **781**, 247 (2007).
- [27] G. Kiss, M. La Cognata, C. Spitaleri, R. Yarmukhamedov, I. Wiedenher, L. Baby, S. Cherubini, A. Cvetinovi, G. D'Agata, P. Figuera, G. Guardo, M. Gulino, S. Hayakawa, I. Indelicato, L. Lamia, M. Lattuada, F. Mud, S. Palmerini, R. Pizzone, G. Rapisarda, S. Romano, M. Sergi, R. Spart, O. Trippella, A. Tumino, M. Anastasiou, S. Kuvin, N. Rijal, B. Schmidt, S. Igamov, S. Sakuta, K. Tursunmakhatov, Z. Flp, G. Gyrky, T. Szcs, Z. Halsz, E. Somorjai, Z. Hons, J. Mrzek, R. Tribble, and A. Mukhamedzhanov, Astrophysical S-factor for the ${}^3\text{He}(\alpha,\gamma){}^7\text{Be}$ reaction via the asymptotic normalization coefficient (ANC) method, *Physics Letters B* **807**, 135606 (2020).
- [28] H. Lüdecke, T. Wan-Tjin, H. Werner, and J. Zimmerer, The reactions ${}^6\text{Li}({}^3\text{He}, {}^3\text{He}_0){}^6\text{Li}$, ${}^6\text{Li}(d,d_0){}^6\text{Li}$, ${}^7\text{Li}(d,d_0){}^7\text{Li}$ and ${}^6\text{Li}({}^3\text{He}, d_{0,1}){}^7\text{Be}$, *Nuclear Physics A* **109**, 676 (1968).
- [29] M. Avrigeanu, W. von Oertzen, U. Fischer, and V. Avrigeanu, Analysis of deuteron elastic scattering on ${}^{6,7}\text{Li}$ up to 50 MeV, *Nuclear Physics A* **759**, 327 (2005).
- [30] A. M. Mukhamedzhanov, H. L. Clark, C. A. Gagliardi, Y. W. Lui, L. Trache, R. E. Tribble, H. M. Xu, X. G. Zhou, V. Burjan, J. Cejpek, V. Kroha, and F. Carstoiu, Asymptotic normalization coefficients for ${}^{10}\text{B}\rightarrow{}^9\text{Be}+p$, *Physical Review C* **56**, 1302 (1997).
- [31] A. Amar and N. Burtebayev, A new analysis of astrophysical s-factor from the experimental data, *Journal of Nuclear Sciences* **1**, 15 (2014).
- [32] L. Blokhintsev, I. Borbely, and E. Dolinsky, *Sov. J. Part. Nucl.* **8**, 485 (1977).
- [33] E. A. George and L. D. Knutson, Determination of the ${}^6\text{Li}\rightarrow\alpha+d$ asymptotic D- to S-state ratio by a restricted phase shift analysis, *Physical Review C* **59**, 598 (1999).
- [34] J. L. Perrenoud and R. M. Devries, Exact finite-range DWBA analysis of multi-nucleon transfer reactions, *Physics Letters B* **36**, 18 (1971).
- [35] A. M. Mukhamedzhanov, R. E. Tribble, and N. K. Timofeyuk, Possibility to determine the astrophysical S factor for the ${}^7\text{Be}(p,\gamma){}^8\text{B}$ radiative capture from analysis of the ${}^7\text{Be}({}^3\text{He},d){}^8\text{B}$ reaction, *Phys. Rev. C* **51**, 3472 (1995).
- [36] R. Yarmukhamedov and L. D. Blokhintsev, Asymptotic Normalization Coefficients (Nuclear Vertex Constants), Three-Body Asymptotic Normalization Functions (On-Shell Vertex Functions) and Nuclear Astrophysics, *Physics of Atomic Nuclei* **81**, 616 (2018).
- [37] S. V. Artemov, I. R. Gulamov, E. A. Zaparov, I. Y. Zotov, and G. K. Nie, Analysis of the reactions $({}^3\text{He}, d)$ on 1p-shell nuclei by a method combining DWBA and dispersion relations, *Physics of Atomic Nuclei* **59**, 428 (1996).
- [38] O. R. Tojiboev, R. Yarmukhamedov, S. V. Artemov, and S. B. Sakuta, Asymptotic normalization coefficients for ${}^7\text{Be}+p\rightarrow{}^8\text{B}$ from the peripheral ${}^7\text{Be}(d,n){}^8\text{B}$ reaction and their astrophysical application, *Physical Review C* **94**, 054616 (2016), arXiv:1602.03637 [nucl-th].
- [39] I. J. Thompson, Coupled reaction channels calculations in nuclear physics, *Computer Physics Reports* **7**, 167 (1988).
- [40] N. Burtebaev, A. D. Duisebaev, B. A. Duisebaev, G. N. Ivanov, and S. B. Sakuta, Elastic and inelastic scattering of 50-MeV α particles by ${}^6\text{Li}$ and ${}^7\text{Li}$ nuclei: The role of exchange effects in anomalous scattering at large angles, *Physics of Atomic Nuclei* **59**, 29 (1996).
- [41] O. F. Nemets, *Nucleon Associations in Atomic Nuclei and Nuclear Reactions with Multi-Nucleon Transfer [in Russian]* (Naukova Dumka, Kiev, 1988).
- [42] K. I. Tursunmakhatov and R. Yarmukhamedov, Determination of the asymptotic normalization coefficient (nuclear vertex constant) for $\alpha + d \rightarrow {}^6\text{Li}$ from the new direct measured $d(\alpha,\gamma){}^6\text{Li}$ data and its implication for extrapolating the $d(\alpha,\gamma){}^6\text{Li}$ astrophysical S factor at Big Bang energies, in *International Journal of Modern Physics Conference Series*, International Journal of Modern Physics Conference Series, Vol. 49 (2019) p. 1960017.
- [43] K. I. Tursunmakhatov, R. Yarmukhamedov, and S. B. Igamov, Asymptotic normalization coefficient for $\alpha+d\rightarrow{}^6\text{Li}$ from the peripheral direct capture $d(\alpha,\gamma){}^6\text{Li}$ reaction and the astrophysical S factor at Big Bang energies, in *European Physical Journal Web of Conferences*, European Physical Journal Web of Conferences, Vol. 227 (2020) p. 02016.
- [44] S. B. Dubovichenko, N. Burtebaev, D. M. Zazulin, Z. K. Kerimkulov, and A. S. A. Amar, Astrophysical S factor for the radiative-capture reaction $p\,{}^6\text{Li}\rightarrow{}^7\text{Be}\gamma$, *Physics of Atomic Nuclei* **74**, 984 (2011).
- [45] S. Cohen and D. Kurath, Spectroscopic factors for the 1p shell, *Nuclear Physics A* **101**, 1 (1967).
- [46] N. Burtebayev, J. T. Burtebayeva, N. V. Glushchenko, Z. K. Kerimkulov, A. Amar, M. Nassurilla, S. B. Sakuta, S. V. Artemov, S. B. Igamov, A. A. Karakhodzhaev, K. Rusek, and S. Kliczewski, Effects of t- and α -transfer on the spectroscopic information from the ${}^6\text{Li}({}^3\text{He},d){}^7\text{Be}$ reaction, *Nuclear Physics A* **909**, 20 (2013).
- [47] F. E. Cecil, D. Ferg, H. Liu, J. C. Scorby, J. A. McNeil, and P. D. Kunz, Radiative capture of protons by light nuclei at low energies, *Nucl. Phys. A* **539**, 75 (1992).